

Characterization and Analysis of LCoS displays: Application to Diffractive Optics

A. Lizana^a, I. Moreno^b, A. Ruiz Márquez^c, C. Iemmi^d, J. Campos^a and M.J. Yzuel^a

^aDept. de Física, Universitat Autònoma de Barcelona, 08193, Bellaterra, Spain

^bDept. de Ciencia de Materiales, Ópt. y Tec. Electrónica, Univ. Miguel Hernández, Elche, Spain

^cDept. de Física, Universidad de Alicante, 03080 Alicante, Spain

^dDept. de Física, Universidad de Buenos Aires, 1428, Buenos Aires, Argentina

ABSTRACT

This work shows a characterization and a polarimetric analysis of a Liquid Crystal on Silicon (LCoS) display, device that works with reflection of the light. We have observed that the optical axis of the LCoS display molecules fluctuates as a function of the time as a consequence of the type of electrical signal addressed to the device. These time fluctuations lead to two different physical phenomena that may decrease the efficiency when addressing diffractive elements to the display: the effective depolarization and the phase-fluctuations phenomena. We have developed a study of these two phenomena and its influence on diffractive elements.

In particular, two different characterization methodologies suitable to obtain the Mueller matrix of the LCoS display are shown. The obtained results are provided and processed to perform a polarimetric study. Next, an intensity or a phase optimization of the LCoS display response is done, in order to obtain configurations of external polarizers and waveplates that allow us to improve the use of this device in optical applications. This study is done as a function of the incident angle and as a function of the wavelength, in order to detect the influence of these parameters on the effective depolarization origin and of the phase-fluctuations. In addition, we have analyzed the influence of the phase-fluctuations phenomena on the efficiency of a phase grating and a digital hologram addressed to the LCoS display.

Keywords: LCD, LCoS display, depolarization, retardance, temporal fluctuations, phase fluctuations.

1. INTRODUCTION

Liquid Crystal Displays (LCDs) are a mature technology that is widespread used in a large number of optical applications due to their capability to work as spatial light modulators. As an example, the LCD are used in adaptive optics [1], optical metrology [2], medical optics [3], holographic data storage [4] or diffractive optics [5]. Different type of LCDs provide diverse manufacturing features: LC material, molecular alignment, effective resolution, pixel size, LC thickness, among others. Recently, a type of LCD, the Liquid Crystal on Silicon (LCoS) display, is being used in diverse applications. The LCoS displays work in reflection, performing the light beam a double pass through the device that leads to more phase-shift than transmissive LCDs with the same LC thickness. This is a very attractive feature in optical applications where the LCD is operating into the phase-only spatial light modulation regime, as frequently happen in diffractive optics applications [6]. Nevertheless, some unpolarized light has been detected [7-9] at the LCoS display reflected beam that has to be taken into account when using them in applications. In addition, the effective depolarization detected depends on different parameters as can be the incident state of polarization, gray level addressed to the LCoS display [7], angle of incidence [10] or wavelength [11].

In Ref. [9], the origin of the effective depolarization detected when working with an Twisted-Nematic (TN) LCoS display in normal incidence and illuminated with a 633.8 nm light beam is studied. In fact, the unpolarized light is related to time-fluctuations of the LC molecules optical axis orientation. In particular, the type of binary signal addressed to the LCoS display is not able to keep still the molecules into a frame period, producing the time-fluctuations phenomena. As the LC is an anisotropy material, time-fluctuations of the LC molecules produces changes of the reflected state of polarization (SoP) as a function on the time. Thus, the temporal average of the SoP variations

(performed, for instance, by CCD cameras and photometers for radiometric measurements) gives the effective depolarization. Further researches have proved that the time-fluctuations on the LC molecules are the origin of other physical phenomena that can adversely affect the efficiency of diffractive elements addressed to the LCoS display: the phase time-fluctuation effect [12].

Here, we present a revision of diverse papers [7,9-12,13] published in the recent years that have been conducted by researchers of the Universitat Autònoma de Barcelona (UAB) in collaboration with researches of the Universidad Miguel Hernandez, the Universidad of Alicante (UA) and the Universidad of Buenos Aires. These papers represent an exhaustive study of an Twisted Nematic LCoS display, very useful for lead to an improvement of applications where the use of LCoS displays is required.

The outline of this work is as follows. In section 2, a polarimetric analysis of a Twisted Nematic LCoS display as a function of different physical parameters is provided. In section 3, a methodology for optimize the intensity and phase response of the LCoS display is presented. Then, in section 4, the effective depolarization and phase fluctuations phenomena and its influence on diffractive elements are revised. Finally, we present some conclusions.

2. POLARIMETRIC ANALYSIS OF THE LCOS DISPLAY

In this section, we show a thoroughly study of some polarimetric properties of a Twisted Nematic (TN) LCoS display. In order to perform the polarimetric analysis, we have characterized the Mueller matrix of the LCoS display as a function of the gray level (GL) and other important physical parameters as the incident angle or the wavelength. For the LCoS display characterization, the Mueller-Stokes (M-S) formalism has been chosen because it is suitable to describe polarizing samples and to deal with depolarization. The LCoS display under analysis is a Philips model X97c3A0, sold as the kit LC-R2500 by Holoeye. The LC-R2500 is a 2.46 cm diagonal reflective LCoS display of the 45° twisted nematic type, with XGA resolution (1024 x 768 pixels), with digital data input and digitally controlled gray scales with 256 gray levels. The pixels are square with a center to center separation of 19 μm and an excellent fill factor of 93%.

The experimental measurement of the LCoS display Mueller matrices has been conducted by means of a characterization method [10] based in the synchronous detection [14] and by using the set-up shown in Fig. 1. Basically, it consists in a polarization state generator (PSG) and a polarization state detector (PSD) properly working. They are formed respectively by a polarizer (LP_1) and a quarter-waveplate (WP_1) and by a quarter-waveplate (WP_2) and a polarizer (LP_2). Then, we take radiometric measurements that correspond to the projection of the polarizing element exiting light beam (for different configurations of the PSG) upon diverse configurations of the PSD. By using the obtained radiometric data, the characterization method previously stated leads to the achievement of the Mueller matrix M of any polarizing sample, and in our case, of the LCoS device. The experiment illumination can be change by using different laser sources (633, 532 and 458 nm) and the LCoS is placed on the top of a rotating platform that enables choosing the incident angle α with a precision of 1°.

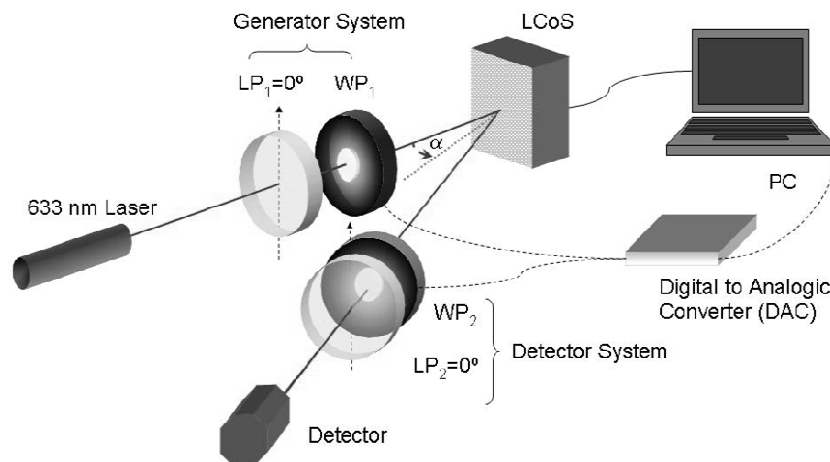


Fig. 1. Set up used to obtain the experimental LCoS Mueller matrix.

2.1 LCoS display polarimetric analysis for quasi-normal incidence and 633 nm light beam

We have performed a first study of the (TN) LCoS display working in quasi-normal incidence (2°) and by illuminating the system with a He-Ne laser (633 nm) [7]. Then, the Mueller matrices of the LCoS display as a function of the gray level (from 0 to 255 gray level in steps of 20) have been measured by following the method previously quoted.

From the experimentally obtained Mueller matrices, some important polarimetric information is available. The last three coefficients of the first row of a Mueller matrix correspond to the diattenuation vector [14] and the three last coefficients of the first column correspond to the polarizance vector [14]. Note that the diattenuation gives a measure of the dependence of the transmittance of an optical element on the incident SoP and the polarizance gives the capability of an optical element to polarize a total unpolarized beam. Moreover, the 3×3 submatrix left when removing the first column and row of the Mueller matrices keep information about the retardance and depolarization values of the polarizing sample that they describe. The obtained results [7] show that the TN LCoS display is a non-diattenuating and non-polarizing element when working under normal incidence and 633nm. In addition, it performs as a linear retarder whose neutral lines orientation and retardance depend on the gray level addressed to the display.

In order to extract some information about the unpolarized light added at the (TN) LCoS display reflected beam, it has been conducted a specific study analyzing this parameter. By experimentally measuring the Stokes parameters of the 633nm light beam we have determined its degree of polarization (DOP) which is defined as [14]:

$$DOP = \frac{\sqrt{S_1^2 + S_2^2 + S_3^2}}{S_0} \quad (1)$$

where S_0 , S_1 , S_2 and S_3 are the Stokes parameters.

Figure 2(a) shows the DoP as a function of six different input states of polarization: linear polarization at 0° of the laboratory vertical (L0), linear polarization at 90° of the lab vertical (L90), linear polarization at 45° (L45), linear polarization at -45° (L135), right-handed circular polarization (CD) and left-handed circular polarization (CL). We see that DOP strongly depends of the gray level addressed to the LCoS display and of the incident state of polarization used.

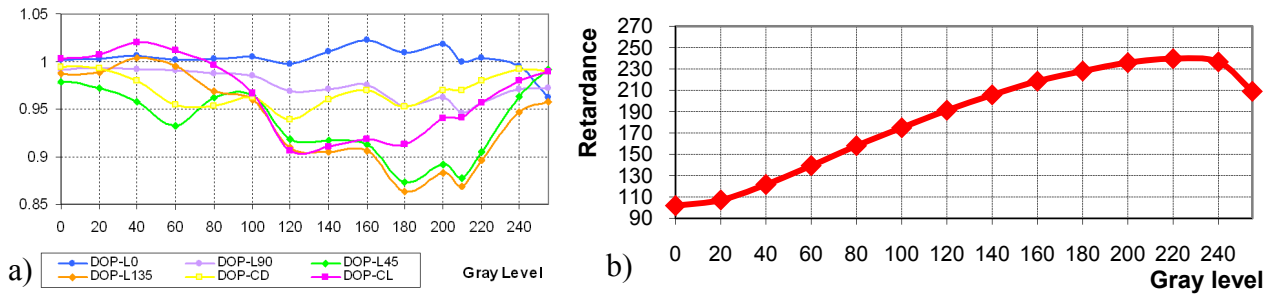


Fig. 2. (a) DoP as a function of the GL and the incident SoP; (b) Retardance values as a function of the GL addressed.

Next, we have analyzed the retardance introduced by the LCoS display. In particular, we have used the combined method presented at Ref. [13], where the Lu-Chipman polar decomposition [14] (based on the polar decomposition theorem [15]) is applied to the Mueller matrix of a (TN) LCoS device, leading to the Jones matrix of the equivalent retarder. The combined method has been applied to the measured Mueller matrices of the LCoS display, reaching the Jones matrices of the equivalent retarder for every gray level used. Then, from the Jones matrices, the eigenvalues and eigenvectors have been calculated, giving the eigenvalues difference the retardance data. The effect produced by the light beam reflexion on the silicon panel has been removed in order to show the pure LCoS display retardance response.

Figure 2(b) shows an evolution of the phase-shift as a function of the gray level. We see that the minimum retardance corresponds to the gray level 0 while the maximum retardance corresponds to the 220 gray level. In addition, the global retardance introduced by the display is about 140 degrees. From this and other results, it has been shown that the LCoS display can be understood as a linear retarder whose retardance and orientation of the neutral lines varies as a function of the gray level.

2.2 LCoS display polarimetric analysis as a function of the wavelength

In this section, the polarimetric study given in section 2.1 is conducted for different wavelengths. In fact, we have used three different wavelengths: 633 nm (He-Ne laser), 532 nm and 458 nm (Argon laser). From the Stokes measurements performed at the LCoS display reflected beam, we can obtain both the degree of polarization (DoP) added at the reflected light, and other polarimetric data such as the diattenuation coefficient as given in [7,14]. First, we have analyzed the DoP dependence with the wavelength used. Figure 3 shows the DoP as a function of the gray level added at the LCoS display reflected beam under quasi-normal incidence and by using the 633 nm (Fig. 3 (a)), 532 nm (Fig. 3(b)) and 458 nm (Fig. 3(c)) wavelengths. Note that the range for the vertical scale is different for the three wavelengths. In every case, the measurements have been done for the incident SoPs used in section 2.1. The DoP strongly depends on the incident state of polarization and the maximum depolarization value obtained clearly increase when using shorter wavelengths. In fact, if we compare the three wavelengths we see that the shorter the wavelength the smaller the DoP.

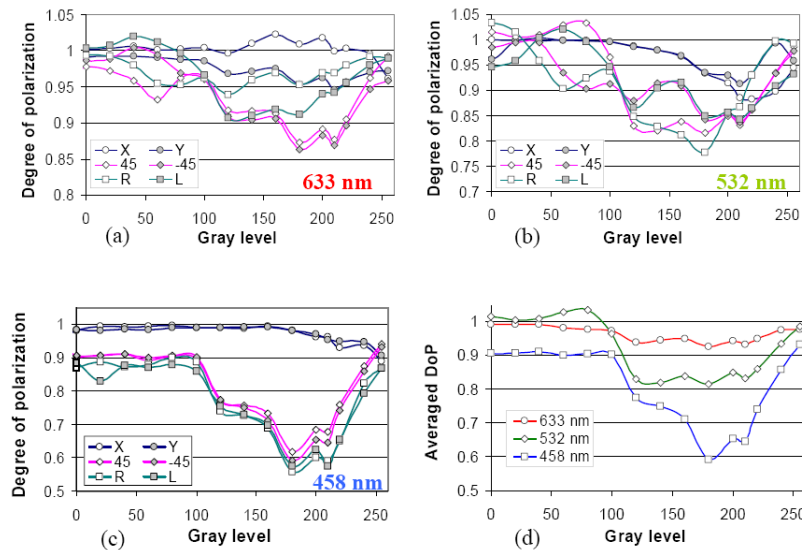


Fig. 3. DOP as a function of different incident SoPs, wavelengths and gray levels.

Moreover, for all the wavelengths, the maximum depolarization is obtained around the 180 gray level, where the LC molecules orientation is strongly affected by the electrical signal addressed. In Fig. 3 (d) we represent the averaged DoP as a function of the gray level and for each of the three wavelengths. This averaged DoP is defined as the arithmetic average calculated from the 6 values measured for the 6 incident SOPs shown in Fig. 3(a), (b) and (c). It can be clearly seen that the DoP decreases for shorter wavelengths, especially for gray levels larger than 100. If we divide the minimum DoP in the graph by the corresponding wavelength we obtain approximately equal ratios (about 1.4), thus we can say that the DoP is inversely related with the wavelength. The diattenuation and polarizance dependence with the wavelength have been also studied showing that the LCoS display is a non diattenuating and non polarizing element independently of the wavelength used. Finally, by following the procedure shown in section 2.1., and by using the Mueller matrices measured for the different GL and for the three wavelengths used, the retardance values have been obtained (Fig. 4).

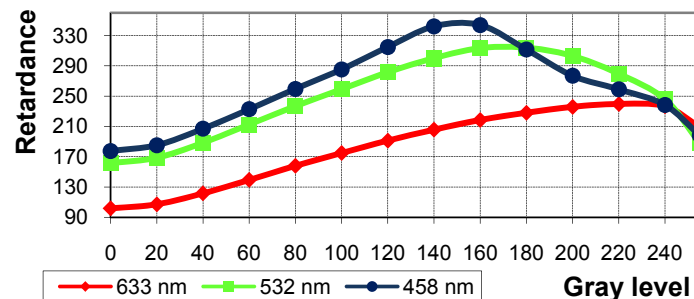


Fig. 4. Retardance as a function of the gray level for three different wavelengths.

The minimum retardance value (100 degrees) is obtained at the 0 GL and with 633 nm. On the other hand, the maximum retardance value is about 350 degree, obtained at the 160 gray level and with 458 nm. By decreasing the wavelength the retardance-shift is increased and the maximum retardance-shift (160 degrees) is obtained when using 458 nm.

2.3 LCoS display polarimetric analysis as a function of the incident angle

A polarimetric study of the LCoS display as a function of the incident angle has been performed. Figure 5 shows the measured DoP as a function of the gray level for various angles of incidence ($\alpha=2^\circ$, 12.5° , 23° , 34° and 45°), calculated from the experimentally measured Stokes parameters. By definition, the DOP takes values from 0 to 1 but in Fig. 5 the y axis has been zoomed in order to show the results more clearly. The results correspond to three input SoPs: linear polarized light at 0° , linear polarized light at 135° and left-handed circular polarized light. In Fig. 5 some DoP values are slightly higher than 1, as a consequence of the instrumental error associated to the intensity measurements in Eq. (1) and its corresponding error propagation. For all the selected incident angles, the DoP depends on the input SoP. Moreover, for a fixed input SoP, there is a quite relevant difference in the DoP evolution as a function of the gray level when changing the incident angle. For quasi-normal incidence (Fig. 5(a)), the reflected light remains fully polarized (DoP close to one) for gray level ranges below 100 or above 240. However, important depolarization effects are detected for gray levels in between 100 and 240, reaching depolarization values higher than 10%.

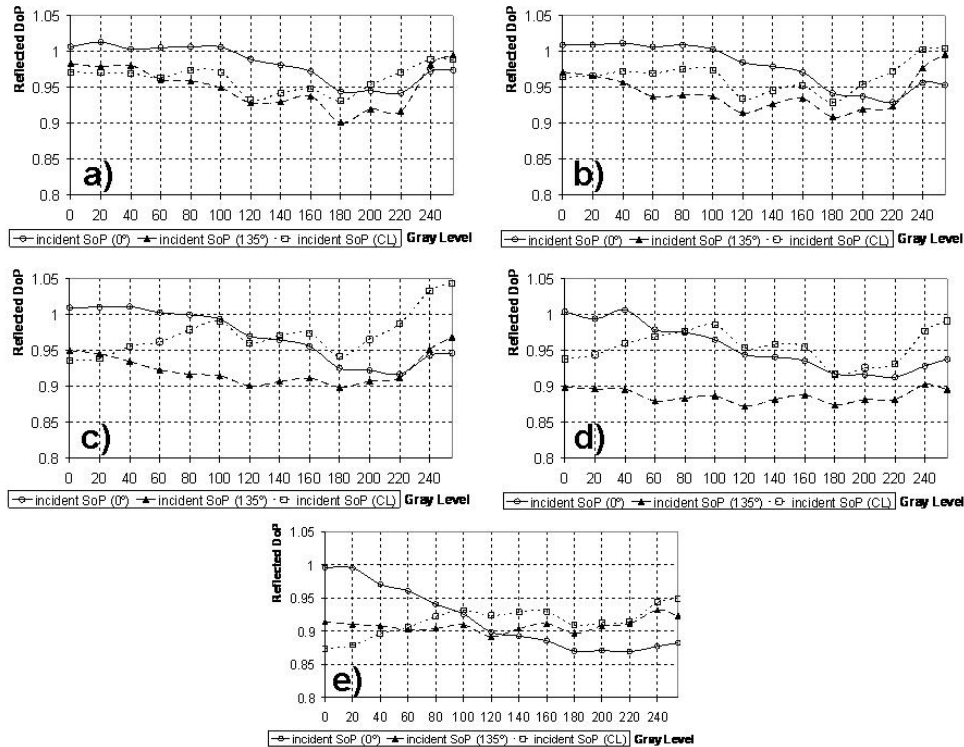


Fig. 5. Degree of polarization as a function of the gray level and for an angle of incidence equal to: a) $\alpha=2^\circ$, b) $\alpha=12.5^\circ$, c) $\alpha=23^\circ$, d) $\alpha=34^\circ$, and e) $\alpha=45^\circ$.

By increasing the incident angle (Figs. 5(b)-5(e)), we detect unpolarized light in the gray level range around gray level 180 (as in the quasi-normal incidence case shown in Fig. 5(a)), but also for higher or lower gray level ranges, where the depolarization increases as the incident angle increases. For instance, for incident angles $\alpha=12.5^\circ$ and $\alpha=23^\circ$ (Figs. 5(b) and 5(c)), depolarization overpass 5%, while it is greater than 10% for incident angles of $\alpha=34^\circ$ and $\alpha=45^\circ$ (Figs. 5(d) and 5(e)). For high incident angles and for some input SoPs, depolarization reaches approximately a 10% along the whole gray level range (black triangles at Fig 5(d) and Fig 5(e)). As we have seen (section 2.1), under normal incidence the LCoS display can be expected to act as linear retarder, whose neutral lines orientation and retardance depend on the addressed voltage. However, when increasing the incident angle, the obtained results have shown that the LCoS may act as an elliptical retarder since the forward and backward paths in the LC layer are no longer coincident. Figure 6 shows

the retardance as a function of the gray level for all the incident angles used along the experience. The retardance values have been calculated from the eigenvalues differences, being the eigenvalues obtained by diagonalizing the Jones matrices of the equivalent retarder. The minimum phase value corresponds to the gray level 0 and an incident angle $\alpha=2^\circ$ (square spots), whereas the maximum phase is obtained for the gray level 240 and $\alpha=45^\circ$ (circular spots). These results show that small incident angles (2° - 12.5°) show a higher phase-shift dynamic range than high incident angles (34° - 45°).

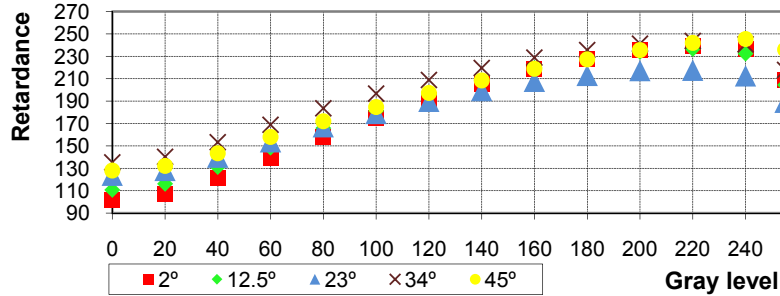


Fig. 6. Retardance as a function of the gray level for different incident angles.

3. PHASE AND INTENSITY LCoS RESPONSE OPTIMIZATION PROCEDURE

In section 2, the Mueller matrices of the LCoS display as a function of the gray level and for different physical parameters have been characterized. From the obtained results some polarimetric information has been provided. Here, by taking advantage of the experimental Mueller matrices we have optimized the intensity and phase response of the LCoS display. The optimization of the intensity and the phase response are obtained by following two different procedures.

The first procedure leads to the LCoS display intensity response optimization. In this case, we use the accurate capability of the LCoS display Mueller matrices to predict the reflected beam SoP when using SoPs corresponding to arbitrary configurations of the PSG and the PSD. Then, by means a numerical searching algorithm, the optimum configuration for the PSG and the PSD providing a specific intensity modulation regime is obtained. To increase the degrees of freedom in this optimization procedure we use a PSG and a PSD capable to cover the whole Poincaré sphere, i.e. every fully polarized SoP. In particular, they are composed of a linear polarizer and a quarter wave plate retarder. There are a series of modulation regimes which are usually of interest, such as maximum intensity contrast modulation or constant amplitude modulation. The modulation regime obtained depends on the figure of merit defined for the numerical search and on the starting values given for the parameters. In our case, the figure of merit used is given below.

$$Q = \frac{1}{\lambda_1 + \lambda_2} \left[\lambda_1 \Delta T + \lambda_2 \left(\frac{\Delta T}{\Delta T + T_m} \right) \right] \quad (2)$$

where the optimized criteria takes into account the variance of the transmission (ΔT) and the minimum transmission value (T_m). Then, by maximizing or minimizing the figure of merit given in Eq. (2), we are operating in the maximum intensity contrast modulation or in the constant amplitude modulation regimes. More details of the intensity optimization procedure can be obtained in [7].

The second procedure leads to the LCoS display phase response optimization. From the measured Mueller matrices the phase modulation can not be a priori evaluated and it has to be measured. However, the use of the Mueller-Stokes formalism in the LCoS display characterization procedure is required because of the effective depolarization values detected when working with these displays (see section 2). Thus, previous Jones matrix approaches to obtain a phase-only response are not directly applicable. However, the possibility of predicting the phase modulation is very desirable, since the phase modulation depth can be increased in configurations with flat but no maximum intensity modulation. We have combined the Mueller and Jones approaches in order to perform a complete characterization of a LCoS display phase response. We apply the polar decomposition [14] of the measured Mueller matrices. This decomposition states that

a general Mueller matrix M can be written as the product of three factors of diattenuation, retardance and depolarization as $M=M_{\Delta}M_R M_D$. As we have seen in section 2, the diattenuation of the LCoS display (independently of the incident angle or wavelength) is negligible, so the polar decomposition can be applied as $M=M_{\Delta}M_R$. Here M_{Δ} and M_R are respectively the depolarization and retardance matrices. Once M_R is calibrated, the equivalent Jones matrix can be calculated and used for the evaluation of the phase modulation. For that purpose, we follow the technique proposed in Ref. [16]. This technique considers that any non-absorbing reciprocal polarization device (for which the LCD is a particular case), can be described by a unimodular unitary Jones matrix, i.e.

$$\mathbf{J}_R = e^{-i\beta} \begin{pmatrix} A & B \\ -B^* & A^* \end{pmatrix} = e^{-i\beta} \begin{pmatrix} A_R - iA_I & B_R - iB_I \\ -B_R - iB_I & A_R + iA_I \end{pmatrix} \quad (3)$$

where $A=A_R-iA_I$ and $B=B_R-iB_I$ are complex parameters (subindices R and I indicate the real and imaginary parts) which depend on the addressed voltage and fulfill the condition $|A|^2 + |B|^2 = 1$. The retarder Mueller matrix equivalent to the Jones matrix in Eq. (3) is given in [13]. Then, with the parameters A and B calibrated and by experimentally measuring the phase β , the global phase response of the LCoS display corresponding to any configuration of the PSG and the PSD can be predicted. Then, a full polarimetric characterization of the display has been achieved. The Mueller matrix accounts for depolarized light, which is necessary to accurately predict the intensity modulation, while the Jones matrix accounts for the phase modulation. Then, the full complex modulation can be predicted and an optimization procedure is applied by minimizing or maximizing the following figure of merit:

$$Q = \frac{1}{\lambda_1 + \lambda_2 + \lambda_3} \left[\lambda_1 \frac{\Delta\tau}{2\pi} + \lambda_2 (1 - \Delta T) + \lambda_3 T_m \right] \quad (4)$$

where the optimized criteria takes into account the variance of the transmission (ΔT), the minimum transmission value (T_m) and the phase-shift $\Delta\tau$.

3.1. Experimental results

In this section we provide some of the experimental results obtained by applying the optimizing procedures given above. Figure 7 shows excellent results obtained for phase-only modulation and for amplitude-only modulation when using 633 nm and quasi-normal incidence (2 degree). Figure 7(a) shows the best results we obtain for phase-only response. We apply an elliptical polarization configuration and we allow a non maximum mean intensity value (around 60%) to achieve a large modulation depth [17,18]. The phase modulation depth reaches 360° giving an almost perfect phase-only modulation. This result is especially relevant since it shows that phase-only diffractive elements can be displayed on this LCoS display with optimal modulation diffraction efficiency, even for a long wavelength as $\lambda=633$ nm. Figure 7(b) shows the intensity and phase modulation for a second configuration, again using an elliptical polarization configuration, to obtain an amplitude-mostly response. A monotonously varying intensity modulation with large contrast is obtained with a minimal coupled phase modulation (less than 60°). In both cases the agreement between experimental and predicted data is excellent. Finally let us note that the DoP is maintained very high in both cases.

Next, figure 8 shows some results corresponding to the phase only regime optimization. In this case, the optimization has been conducted in quasi-normal incidence (2 degree) and for two different wavelengths: 532 nm (Fig. 8(a)) and 458 nm (Fig. 8(b)). Figure 8(a) corresponds to a configuration optimized for $\lambda=532$ nm, using an elliptical polarization light. We see an almost constant intensity response accompanied with a phase shift of 2π . Furthermore, the DoP is almost equal to one as a function of the gray level and we can consider that we are dealing with fully polarized light. The profiles for the intensity and the phase shift modulations obtained in figure 8(a) are similar to the ones obtained in figure 7(a), when optimizing for $\lambda=633$ nm, but for 532 nm we obtain a higher average intensity value. Therefore, by optimizing the response for 532nm we obtain similar values for phase shift that the ones obtained with 633 nm but with an increase of the intensity values. Next, Fig. 8(b) shows the system response corresponding to a configuration optimized for $\lambda=458$ nm and using elliptically polarized light. In this case, we have allowed in our optimization procedure to decrease the minimum intensity value when optimizing for 458 nm. We have obtained an almost constant intensity response as a function of the gray level accompanied with a phase shift higher than 3π . However, there is again some unpolarized light in some gray levels. Nevertheless, in terms of phase shift response, we see that using $\lambda=458$ nm we obtain more phase

shift modulation than when using the previous two wavelengths. We have also tested the configuration optimized for 633nm (Fig.7(a)) with different wavelengths. For these wavelengths, the configuration is not optimal anymore. In fact, the phase-only response is degraded by a coupled intensity modulation and by an increase of the depolarization for high gray levels. Then, a characterization of the LCoS display and an optimization of its intensity and phase response is required for every wavelength used.

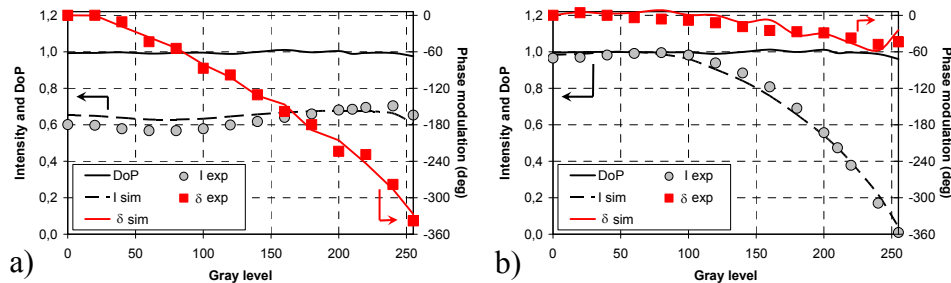


Fig. 7. (a) DoP, intensity and phase modulation for phase-only response. (b) DoP, intensity and phase modulation for amplitude-only response. Lines indicate predictions and symbols experimental data.

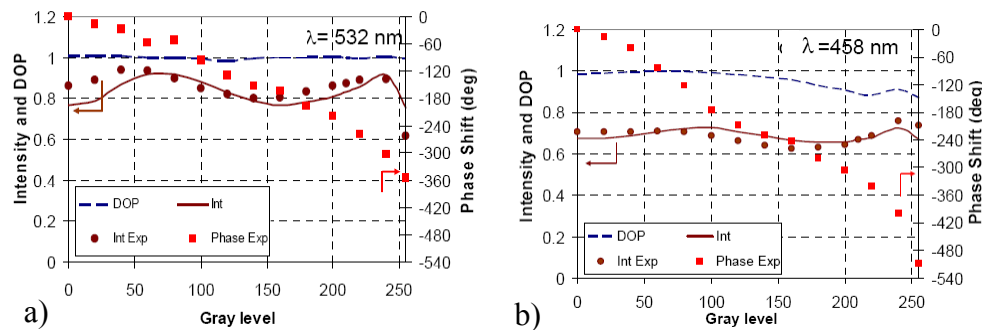


Fig. 8. (a) DoP, intensity and phase modulation in the configuration for phase-only response. (b) DoP, intensity and phase modulation in the configuration for amplitude-only response. Lines indicate predictions and symbols experimental data.

The LCoS display response has been optimized as a function of different incident angles. Figure 9 shows some results obtained for the phase-only modulation regime and for 633nm. On one hand, Fig. 9(a) shows a very constant intensity response (black line and circles) as a function of the gray level for an incident angle equal to $\alpha=12.5^\circ$. Moreover, we obtain almost 2π phase-shift (dotted line and squares). Therefore, the modulation response optimization with $\alpha=12.5^\circ$ provides similar results to those obtained with $\alpha=2^\circ$ (Fig. 7(a)). Thus, for a small range of incident angles (around 10°) a single optimization is enough. On the other hand, Fig. 9(b) ($\alpha=45^\circ$) gives also a constant intensity response but the phase-shift is significantly shorter (only slightly over 240°) than the obtained at quasi-normal incidence (Fig. 7(a)). Therefore, even by optimizing the LCoS display phase modulation response at high incident angles, the results remain worse than the obtained at low incident angles. This result is in agreement with Fig. 6, where the retardance-shift between the equivalent retarder eigenvectors is higher for quasi-normal incidence than for oblique incidence.

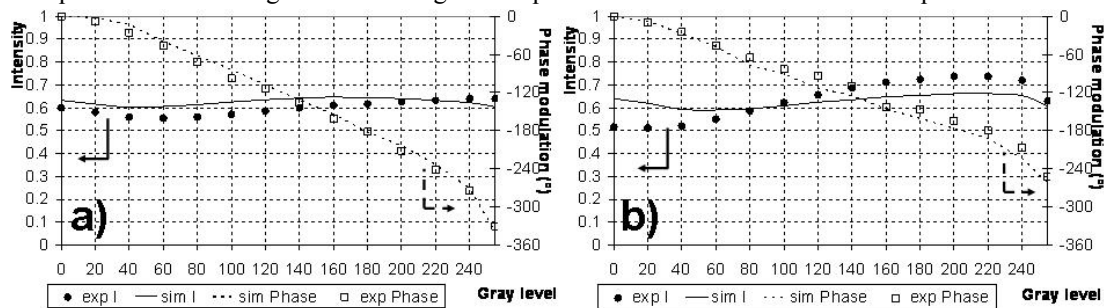


Fig. 9. Phase modulation optimization when using an incident angle equal to: a) $\alpha=12.5^\circ$; b) $\alpha=45^\circ$.

4. TEMPORAL FLUCTUATIONS: DEPOLARIZATION AND PHASE FLUCTUATIONS

In this section, the effective depolarization and the phase fluctuations phenomena are revised. The binary electrical signal corresponding to some gray levels addressed to the LCoS display is not able to keep still the LC molecules. Time fluctuations of the LC molecules may change the exiting SoP and in temporal average, it gives the effective depolarization values. Moreover, the effective depolarization value is increased when increasing the amplitude of the LC molecules fluctuations or when increasing the contrast response of the LCoS display. The temporal average origin of the effective depolarization can be demonstrated by analyzing the SoP of the reflected beam instantaneously (very fast measurements) or as a function of the time (averaged measurements). Experimentally, it can be done by performing the Stokes measurements considering two different integration times that may represent two different detectors. With a photodetector monitorized onto an oscilloscope we can take fast measurements (in our case each 0.02 ms). Using this integration interval, the fluctuations in the intensity of the reflected beam can be time-resolved (they show variations in the order of ms), and we can consider these as instantaneous measurements. On the other hand, in many applications the detector will be a CCD camera that will capture only few images per second. Then, the integration time will be much higher than the optical intensity fluctuations period. In this case, the measured intensity will be the magnitude averaged along several periods, and the state of polarization will significantly change along this integration time. In the first case (fast detector), and with a proper synchronization of the detected signals, the Stokes parameters can be deduced from the measured intensities as [19,20]:

$$\begin{pmatrix} S_0(t) \\ S_1(t) \\ S_2(t) \\ S_3(t) \end{pmatrix} = \begin{pmatrix} I_x(t) + I_y(t) \\ I_x(t) - I_y(t) \\ I_{45}(t) - I_{-45}(t) \\ I_R(t) - I_L(t) \end{pmatrix} \quad (5)$$

where t denotes the time, and I_x , I_y , I_{45} , I_{-45} , I_R and I_L are respectively the intensities measured at the exit of the PSD from the projection of the reflected beam SOP onto the six corresponding SOPs (linear states X, Y, 45, -45, and circular states R and L), for which the PSD is configured. By taking into account Eq. (1), the corresponding degree of polarization is calculated as

$$\text{DoP}(t) = \frac{\sqrt{S_1^2(t) + S_2^2(t) + S_3^2(t)}}{S_0(t)} \quad (6)$$

On the other hand, when using a slow detector, like a CCD, the measured magnitudes will be the averaged intensities. Then the corresponding Stokes vector will be given by

$$\begin{pmatrix} S_0 \\ S_1 \\ S_2 \\ S_3 \end{pmatrix} = \begin{pmatrix} \bar{I}_x + \bar{I}_y \\ \bar{I}_x - \bar{I}_y \\ \bar{I}_{45} - \bar{I}_{-45} \\ \bar{I}_R - \bar{I}_L \end{pmatrix} = \begin{pmatrix} \langle S_0(t) \rangle \\ \langle S_1(t) \rangle \\ \langle S_2(t) \rangle \\ \langle S_3(t) \rangle \end{pmatrix} \quad (7)$$

where the symbol $\langle \rangle$ denotes time averaging on the detector. The corresponding degree of polarization is:

$$\text{DoP} = \frac{\sqrt{S_1^2 + S_2^2 + S_3^2}}{S_0} \neq \langle \text{DoP}(t) \rangle \quad (8)$$

The Stokes parameters measured with the slow detector are the mean averaged value of the Stokes parameters measured with the fast detector. The effective DoP measured with the slow detector differs from the value calculated by averaging the corresponding instantaneous values measured with the fast detector (Eq.8). This is due to the non linear relation in the definition of DoP as a function of the Stokes parameters. We have experimentally measured DoP of the LCoS display reflected beam for different input SoPs (linear states X, Y, 45, -45, 30 and circular states R and L) in two different ways. One hand, the DoP has been calculated from intensity measured performed with a slow detector, and then this DoP value comes from the average of the Stokes vectors. Let us call it DoP (from ASP). On the other hand, we have measured the instantaneously Stokes parameters (ISP) and then, the instantaneous DoPs values. Finally, the mean of the instantaneous DoPs values (MDoP) is calculated. The set-ups used for the corresponding measurements are given in Ref. [9]. The obtained results are shown in Fig. 10. We see that the DoP (from ASP) values, in all cases present a non negligible

amount of depolarization, since DoP is clearly less than one. On the other hand, we see that the MDoP (from ISP) are all very close to one, denoting that the reflected beam is maintained fully polarized if time resolved measurements are considered. The DoP obtained from ASPs exhibits lower values than one, as we expected. This indicates that the depolarization effect measured with slow detectors is due to the rapid fluctuation in the state of polarization. Therefore, to a certain extent, and for applications where the final element is a slow integration detector, the LCoS display could be considered as partially performing a time averaging depolarization, in a way similar to how existing time averaging depolarizers work [21].

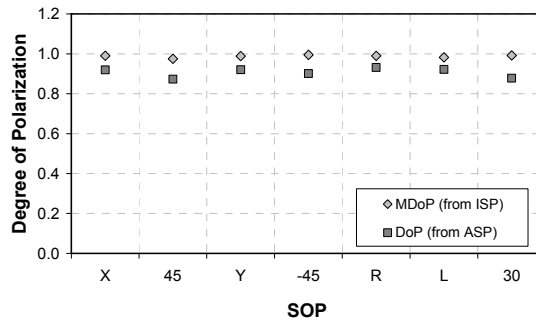


Fig. 10. MDoP (rhombus) and DoP (squares) for different incident SoPs.

Finally, we have detected other physical phenomena related to the LC molecules fluctuations: the time-fluctuations of the phase [12]. It is important to take into account the phase-fluctuations effect because it can adversely affect in some applications, for instance, in diffractive optics where it can decrease the efficiency of the diffractive elements. To prove this effect, we have addressed three different binary gratings to the LCoS display and we have measured the intensity as a function of the time of the zero and first diffracted orders. In particular, the binary gratings used have been addressed with the gray levels (0,120), (0,211) and (0,255). The set-up used is given in Ref. [12] and the obtained results are plotted in Fig. 11 (a)-(c). In addition, Fig. 11 (d) gives the phase modulation as a function of the time obtained from the intensity measurements of the diffracted orders. Figure 11 shows that in all cases fluctuations appear in the intensity measurements (Fig. 11(a)-(c)), and as a consequence in the phase modulation (Fig. 11(d)). Particularly interesting is the case for the grating (0,211) (Fig. 11(b)), where the mean phase difference is equal to 180° , but it is accompanied with a great fluctuation of almost 120° (Fig. 11(d)). These results are in agreement with those in Ref. [9], where the highest depolarization effect was observed around gray level 180. In both cases, the depolarization effect and the phase modulation fluctuation are originated from fluctuations in the orientation of the LC molecules, which appear to be the largest for this range of gray levels in our display.

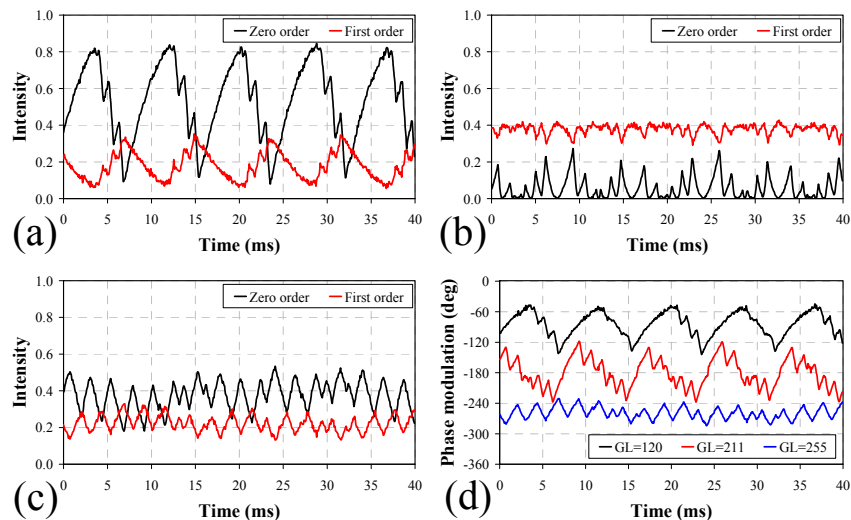


Fig. 11. Intensity measurements at the zero and first diffraction orders for binary diffraction gratings with GL (a) (0,120), (b) (0,211) and (c) (0,255). (d) Instantaneous phase values as a function of time for different GL.

Finally, we have analyzed the effect of the phase fluctuations phenomena in the diffraction efficiency of diffractive optical elements (DOE). Because of the phase fluctuations, the diffraction efficiency of displayed DOEs will also fluctuate. We have tested the effect on two basic binary diffractive optical elements, with average phase levels $0 - \pi$. The results in Fig. 11(d) show that this phase difference can be obtained (for the average phase values) for gray levels $GL=0$ and $GL=211$. First, we have addressed a binary phase-only grating. In this case, a power of 40% in the first order and a zero order vanished are expected. The results are shown in Fig. 12(a), which shows the typical diffraction orders generated by the grating. However, although the ± 1 orders are stronger, the zero order does not vanish as a consequence of the phase fluctuations. Next, we displayed a binary phase computer generated hologram designed to reconstruct a butterfly. The results are shown in Fig. 12(b). A linear phase along the diagonal direction is added to spatially separate the reconstruction of the different terms. In this way we separate the zero and ± 1 orders. The butterfly is reconstructed in the ± 1 orders with an efficiency equivalent to that of the first diffraction order in Fig. 12(a). The -1 order results in an inverted version of the butterfly, as expected. Again, the zero order term appears in the form of a light peak located on axis, originated from the time fluctuations in the phase modulation.

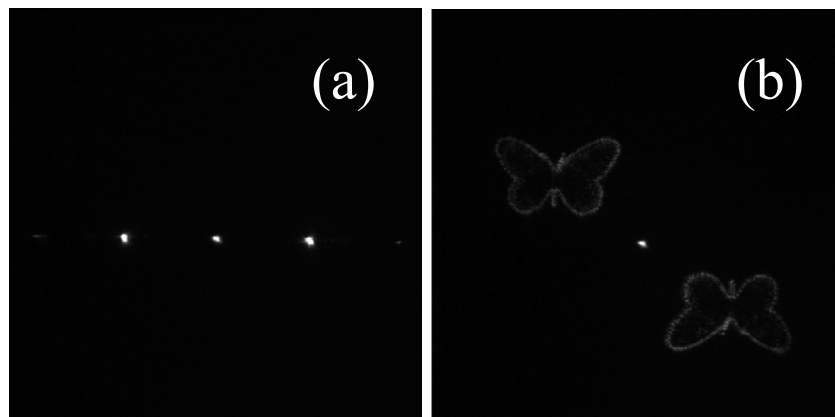


Fig. 12. Fourier transform spectrum captured with the CCD camera when a binary DOE is displayed onto the LCoS display with gray levels (0,211) (mean phase difference of π radians). (a) Binary diffraction grating. (b) Computer generated hologram designed to reconstruct a butterfly.

CONCLUSIONS

Liquid Crystal on Silicon displays are LCDs that work in reflection. These devices are widespread used in optical applications due to its capability to work as spatial light modulators. This work presents a review of some works dealing with LCoS displays that have been conducted by researchers of the Universitat Autònoma de Barcelona in collaboration with researches of the Universidad Miguel Hernandez, the Universidad of Alicante and the Universidad of Buenos Aires.

In particular, we present an extensive study of the polarimetric properties (as effective depolarization, retardance, diattenuation and polarizance) of a Twisted Nematic (TN) LCoS display as a function of different physical parameters as the gray level, the incident angle of the wavelength. Moreover, a methodology for the optimization of the (TN) LCoS display intensity and phase response is provided. Finally, an experimental prove of the phase fluctuations phenomena and its influence in the efficiency of diffractive elements generated by using the LCoS display is also provided.

Acknowledgments: We acknowledge financial support from Spanish Ministerio de Educación (FIS2006-13037-C02-01 and 02) and Generalitat de Catalunya (2006PIV00011). C. Iemmi gratefully acknowledges the support of Universidad de Buenos Aires and CONICET (Argentina).

REFERENCES

- [1] R. Dou and M.K. Giles, "Closed-loop adaptive optics system with a liquid crystal television as a phase retarder", Opt. Letters, 20, p. 1583-1585 (1995).

- [2] W. Osten, C. Kohler and Liesener, "Evaluation and application of spatial light modulators for optical metrology", *Opt. Pura Apl.* 38, p. 71-81 (2005).
- [3] K.M. Twietmeyer, R.A. Chipman, A.E. Elsner, Y. Zhao and D. VanNasdale, "Mueller matrix retinal imager with optimized polarization conditions", *Opt. Express* 16, p. 21339-21354 (2008).
- [4] H. J. Coufal, D. Psaltis and B. T. Sincerbox, *Holographic Data Storage*, (Springer-Verlag, Berlin, 2000).
- [5] P.J. Turunen and F. Wyrowski, *Diffractive Optics for Industrial and Commercial Applications*, (Akademie Verlag, Berlin, 1997).
- [6] M.O. Freeman, Hsi-Fu Shih, Y.C. Lee and J.J. Ju, "LCD diffractive element design to handle multiple disk thicknesses", *SPIE proceeding series*, vol. 4081, pp. 256-266 (2000).
- [7] A. Márquez, I. Moreno, C. Iemmi, A. Lizana, J. Campos and M.J. Yzuel, "Mueller-Stokes characterization and optimization of a liquid crystal on silicon display showing depolarization", *Opt. Express* 16, p. 1669-1685 (2008).
- [8] J.E. Wolfe and R.A. Chipman, "Polarimetric characterization of liquid-crystal-on-silicon panels," *Appl. Opt.* 45, p. 1688-1703 (2006).
- [9] A. Lizana, I. Moreno, C. Iemmi, A. Márquez, J. Campos and M.J. Yzuel, "Time-resolved Mueller matrix analysis of a liquid crystal on silicon display," *Appl. Opt.* 47, p.4267-4274 (2008).
- [10] A. Lizana, N. Martín, M. Estapé, E. Fernández, I. Moreno, A. Márquez, C. Iemmi, J. Campos and M.J. Yzuel, "Influence of the incident angle in the performance of Liquid Crystal on Silicon displays", *Opt. Express*, Vol. 17 (10), 8491-8505, (2009).
- [11] A. Lizana, A. Márquez, I. Moreno, C. Iemmi, J. Campos and M. J. Yzuel, "Wavelength dependence of polarimetric and phase-shift characterization of a liquid crystal on silicon display", *J. Eur. Opt. Soc. - Rapid Pub.* 3, p. 08011 1-6 (2008).
- [12] A. Lizana, I. Moreno, A. Márquez, C. Iemmi, E. Fernández, J. Campos and M. J. Yzuel, "Time fluctuations of the phase modulation in a liquid crystal on silicon display: characterization and effects in diffractive optics," *Opt. Express* 16, 16711-16722 (2008).
- [13] I. Moreno, A. Lizana, J. Campos, A. Márquez, C. Iemmi and M. J. Yzuel, "Combined Mueller and Jones matrix method for the evaluation of the complex modulation in a liquid-crystal-on-silicon display," *Opt. Lett.* 33, p.627-629 (2008).
- [14] D. Goldstein, *Polarized Light*, (Marcel Dekker, NY, 2003).
- [15] P. Lancaster and M. Tismenetsky, *The Theory of Matrices*, (2nd Ed. Academic, San Diego, 1985).
- [16] I. Moreno, P. Velásquez, C. R. Fernández-Pousa, M. M. Sánchez-López and F. Mateos, *J. Appl. Phys.* 94, 3697-3702 (2003).
- [17] A. Márquez, C. Iemmi, I. Moreno, J. A. Davis, J. Campos and M. J. Yzuel, "Quantitative prediction of the modulation behavior of twisted nematic liquid crystal displays based on a simple physical model", *Opt. Eng.* 40, 2558-2564 (2001).
- [18] J.A. Davis, J. Nicolás and A. Márquez, "Phasor analysis of eigenvectors generated in liquid crystal displays", *Appl. Opt.* 41, 4579-4584 (2002).
- [19] I. Moreno, P. Velásquez, C. R. Fernández-Pousa, M. M. Sánchez-López and F. Mateos, "Jones matrix method for predicting and optimizing the optical modulation properties of a liquid-crystal display," *J. Appl. Phys.* 94, 3697-3702 (2003).
- [20] S. Huard, *Polarization of Light*, John Wiley and Sons, New York (1997).
- [21] E. Collet, "Optical depolarizers and scramblers", Chap. 12 in *Polarized Light in Fiber Optics*, The PolaWave Group, Lincroft, New Jersey (2003).